

Very high-resolution radio observations of HzRGs

M. A. PÉREZ-TORRES¹, C. DE BREUCK², W. VAN BREUGEL³, and G. MILEY⁴

¹ Instituto de Astrofísica de Andalucía - CSIC, Apdo. Correos 3004, E-18080 Granada, Spain

² European Southern Observatory, Karl Schwarzschild Straße 2, D-85748 Garching, Germany

³ Lawrence Livermore National Laboratory, PO Box 808, Livermore, CA 94550, USA

⁴ Leiden Observatory, University of Leiden, PO Box 9513, Leiden, 2300 RA, The Netherlands

Received; accepted; published online

Abstract. We report on first results of an ongoing effort to image a small sample of high-redshift radio galaxies (HzRGs) with milliarcsecond (mas) resolution, using very-long-baseline interferometry (VLBI) techniques. Here, we present 1.7 and 5.0 GHz VLBA observations of B3 J2330+3927, a radio galaxy at $z=3.087$. Those observations, combined with 8.4 GHz VLA-A observations, have helped us interpret the source radio morphology, and most of our results have already been published (Pérez-Torres & De Breuck 2005). In particular, we pinpointed the core of the radio galaxy, and also detected both radio lobes, which have a very asymmetric flux density ratio, $R > 11$. Contrary to what is seen in other radio galaxies, it is the radio lobe furthest from the nucleus which is the brightest. Almost all of the Ly-alpha emission is seen between the nucleus and the furthest radio lobe, which is also unlike all other radio galaxies. The values of radio lobe distance ratio, and flux density ratio, as well as the fraction of core emission make of B3 J2330+3927 an extremely asymmetric source, and challenges unification models that explain the differences between quasars and radio galaxies as due to orientation effects.

Key words: galaxies: high redshift – galaxies: jets – galaxies: individual (B3 J2330+3927)

©0000 WILEY-VCH Verlag GmbH & Co. KGaA, Weinheim

1. Introduction

The combination of high-resolution radio observations with high angular resolution optical imaging and, more recently, with X-ray imaging, contributes important information to the study of high-redshift radio galaxies (HzRGs, $z > 2$). For example, McCarthy et al. (1987) and Chambers et al. (1987) have clearly illustrated, by using radio, optical and UV observations the existence of a radio-aligned optical line-emission and UV-continuum, strongly supporting the proposed scenario where a young radio AGN having powerful jets and ionizing radiation can dramatically affect the environment of their forming host galaxies. This scenario has been confirmed by recent discoveries of similarly radio-aligned X-ray emission (e.g., Carilli et al. 2002, Scharf et al. 2003).

High-resolution radio data is also of high relevance in studying the interaction of the radio sources with gas in the putative forming galaxy (e.g., 100 kpc-scale Ly- α halos). In particular, the comparison of high-resolution radio and Ly- α images may point to the interaction between the propagating jet and the surrounding interstellar medium, and constrain

the relative importance of jet-induced star formation, shock ionized gas, and dust/electron scattering in forming the observed optical galaxies.

2. VLBI observations of HzRGs

The enormous distances at which HzRGs lie, make it necessary to go from 'high-resolution' to 'very high-resolution' radio observations, if we are to better understand the physics of the individual objects subject to study. We have thus started a radio programme aimed at studying with VLBI a small sample of high-redshift radio galaxies whose peculiar radio morphologies suggest that strong interactions with their surrounding medium are taking place, based on existing high-resolution HST optical imaging. Our strategy is to carry out detailed morphological comparisons of radio and optical continua for the sources of the sample, with the goal of distinguishing among the effects of jet-induced star formation. VLBI images, of higher resolution than HST optical images, can delineate the shocks associated with the propagation of the jets, and even pinpoint potential sites of star formation. If there is no one-to-one relationship between the radio and optical morphologies, this will likely indicate that scattering is

the dominant mechanism. In addition, a detailed morphological comparison with the Ly- α maps may be used to study the interaction between the propagating jet and the surrounding primeval interstellar medium (ISM). This ISM may cause the jets to bend and decollimate, and affect the ionization and kinematics of the gas.

Our sample consists of four sources: B3 J2330+3927 ($z = 3.1$), B2 0902+34 ($z = 3.4$), 4C 41.17 ($z = 3.8$), and TN J1338-1942 ($z = 4.1$). We observed B3 J2330+3927 on November-December 2004, using the VLBA at 1.7 and 5.0 GHz. 4C 41.17 and B2 0902+34 have been observed in June 2005 using simultaneously the European VLBI Network (EVN) and the Multi-Element Radio-Linked Interferometer Network (MERLIN) observations, and the data reduction is underway. Here, we report results from our observing campaign on B3 J2330+3927. Throughout the paper, we have assumed a Λ -dominated universe with $\Omega_M = 0.3$, $\Omega_\Lambda = 0.7$, and $H_0 = 65 \text{ km s}^{-1} \text{ Mpc}^{-1}$. At $z = 3.087$, $1''$ corresponds to 8.2 kpc.

3. B3 J2330+3927: A case study

The radio galaxy B3 J2330+3927 has been studied at several frequencies by De Breuck et al. (2003), hereafter DB03. The 8.4 GHz VLA observations of DB03 (see Fig. 1) showed that B3 J2330+3927 is a $\sim 2''$ wide source consisting of three radio components, located in between two optical (K -band) objects (a and b). The triple radio morphology in the VLA A-array 8.4 GHz map is reminiscent of other radio galaxies, where the host galaxy is located at the position of the central radio component. Optical and near-IR Keck spectroscopy of B3 J2330+3927 show AGN emission lines from object a , while object b has a velocity offset of +1500 km/s with respect to object a . However, no emission lines are seen at the position of the central radio source. Because the relative astrometric uncertainty is $< 0''.4$, the central radio component cannot be reconciled with the AGN in object a . De Breuck et al. (2003) proposed two interpretations: (i) the northern radio component is the core, implying a one-sided jet radio morphology, or (ii) the marginally resolved central radio source is the radio core, and the AGN is heavily obscured at this position. The latter explanation would be inconsistent with the peak of the CO emission, which coincides with object a . As we show below, only the higher angular resolution provided by VLBI, together with spectral index information, has been able to uniquely point to the correct AGN identification.

We have recently published (Pérez-Torres & De Breuck 2005; hereafter PTDB) new results on B3 J2330+3927, based on Very Long Baseline Array (VLBA) at 1.7 and 5 GHz carried out on 2004 November 29 and December 9, respectively, as well as on archival 1.4 GHz VLA data and our reanalysis of the 8.4 GHz VLA data of B3 J2330+3927 (DB03). We analyzed the radio data using the Astronomical Image Processing System (AIPS). We used standard phase self-calibration techniques within AIPS to obtain the images shown in Fig. 2. We give in the following section an account of some of the results obtained in PTDB, and refer the reader to that paper

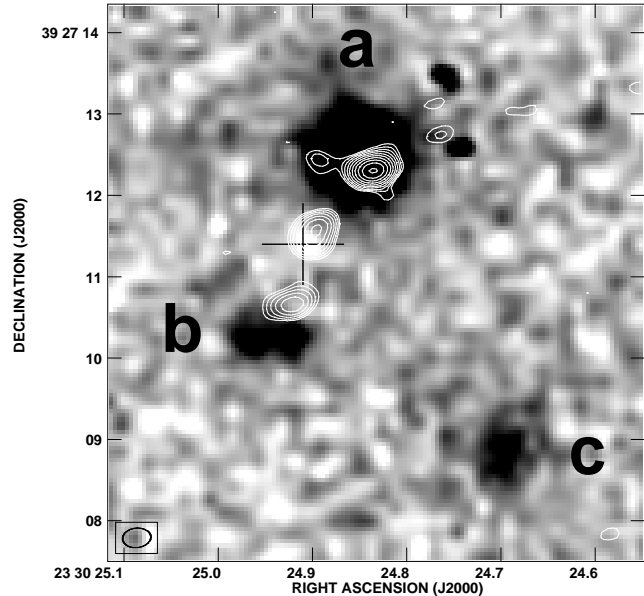


Fig. 1. 8.4 GHz VLA A-array image of B3 J2330+3927 overlaid on a NIRC/Keck K -band image (from De Breuck et al. 2003). The optical AGN emission lines are located at the position of the bright object a , while the radio morphology suggests the core to be located in between objects a and b . The cross indicates the NVSS position.

for technical details, as well as for a thorough account of the results obtained from our VLBA observations.

4. Results

Figure 2 shows the reanalyzed 8.4 GHz VLA data on B3 J2330+3927, with the archival 1.4 GHz data overlaid. In addition to the three components identified by DB03, we also detect a faint component on the northwestern side of object a . In the following, we call these components A, B, C, and N, as identified in Fig. 1. The newly found component, A, shows for the first time the detection of the counter-jet in B3 J2330+3927, providing support for the interpretation that the radio component N, coincident with object a , is the radio core.

We mapped the entire region, encompassing objects A through C, using the VLBA. Only components N and B were detected, both at 1.7 and 5.0 GHz. The left panel in Fig. 2 shows the 8.4 GHz map of these components, while the right panel displays a blow-up of component N to show the VLBA data at their full resolution (for a detailed report of those observations see PTDB). Our 1.7 GHz VLBA data (contours) shows that region N consists of a compact ($\lesssim 4$ mas in size) core-jet, N1, and a jet feature, N2. Our 5.0 GHz VLBA data only detected component N1, which has a spectral index $\alpha_{5.0}^{1.7} = -0.2 \pm 0.1$. Component N2 was detected at 1.7 GHz, but not at 5.0 GHz, indicating that $\alpha_{5.0}^{1.7} \lesssim -0.9$. Because component N1 has the flattest spectral index of all components in our VLBA images, we identified it as the long-sought radio core of B3 J2330+3927.

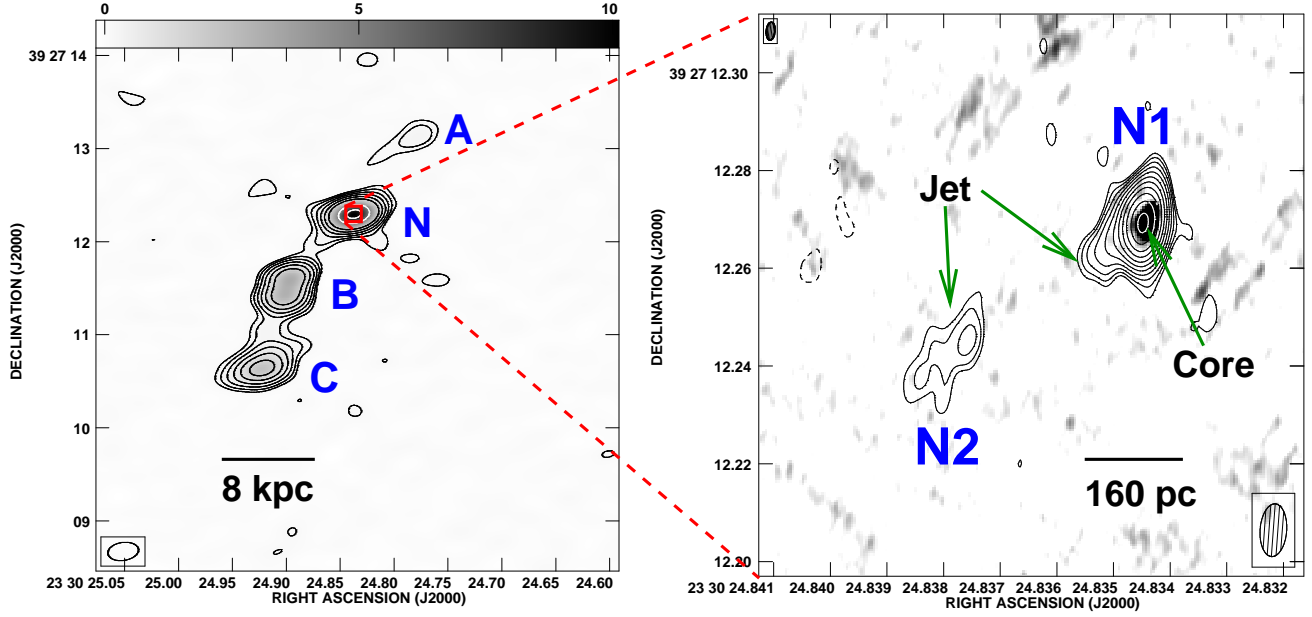


Fig. 2. *Left:* 8.4 GHz VLA A-array, uniformly weighted image of B3 J2330+3927 on 30 March 2002. The contour scheme is a geometric progression in $\sqrt{3}$. The first contour level is at $0.12 \text{ mJy beam}^{-1}$. The synthesized beam is $0''.3 \times 0''.2$ at position angle -82° . The total cleaned flux density in the image is $\approx 21.4 \text{ mJy}$ and the image off-source rms $\sim 40 \mu\text{Jy/beam}$ (see left panel of Fig. 2). Note the detection of component A, the faint, near radio lobe. *Right:* VLBA image of component N, as obtained from our VLBA observations at 1.7 GHz (contours) and 5.0 GHz (greyscale). Contour levels are a geometric progression in $\sqrt{2}$, with the first contour starting at $0.1 \text{ mJy beam}^{-1}$. The off-source rms noise in the image was of $\sim 60 \mu\text{Jy}$ at both 1.7 and 5.0 GHz. Note the protrusion southeast of component N1, which corresponds to the jet emanating from the radio core.

The identification of the core with component N1 confirms that C and the newly found component, A, are the radio lobes of B3 J2330+3927. Indeed, wide-field ($1^\circ \times 1^\circ$), deep 1.4 GHz VLA imaging (PTDB) excludes the presence of significant radio emission beyond component A, and no other components are seen in the WENSS or NVSS. Thus, our identification of component A with the outer radio lobe is robust. Now, from the 8.4 GHz reanalyzed data, we find that (a) the fraction of emission from the nuclear component is $f_c = 0.50$; (b) the ratio of the core-lobe distances is $Q = (N1 - C)/(N1 - A) \approx 1.9$; and (c) the ratio of the flux densities of the further lobe to that of the closer lobe is $R = S_C/S_A \gtrsim 11$.

5. Discussion

The combined use of VLA and VLBA data, along with the existing multiwavelength observations, allows us to draw a consistent picture of the radio structure of B3 J2330+3927, revealing also several puzzling properties: the compact, flat spectrum ($\alpha \sim -0.2$) component N, is the radio core of B3 J2330+3927, and is located at the position of the optical/near-IR type II AGN and the peak of the CO(4-3) emission. The 8.4 GHz VLA image reveals a previously undetected, faint counterjet (A), confirmed by very deep, 1.4 GHz VLA observations, and implying that A and C are the closer and farther lobes, respectively, of the radio galaxy. The radio source properties are extremely asymmetric, as indicated by the values of Q , R , and f_c .

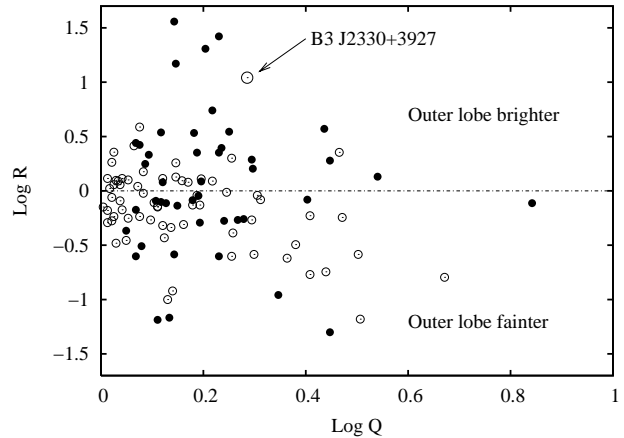


Fig. 3. The $\log Q$ - $\log R$ diagram for the radio galaxies (open circles) and quasars (solid circles) of the Saikia et al. (2001) sample, along with our case study source, B3 J2330+3927.

Best et al. (1995) have shown convincing evidence that quasars have more asymmetric radio morphologies than radio galaxies, and this finding is consistent with expectations of the unified model, namely that quasars and radio galaxies are intrinsically similar, but quasars are observed when the radio jet axis of the source is within 45° of the line of sight (Barthel 1989). We show in Fig. 3 the $\log Q$ - $\log R$ diagram for the 78 radio galaxies and quasars from the 3CR and S4 samples selected by Saikia et al. (1995, 2001). Note that there are no radio galaxies in the diagram with $\log R \gtrsim 0.6$,

in contrast with quasars. B3 J2330+3927, with a value of $\log R=1.04$, is thus a very bizarre radio galaxy, and looks more like a quasar. Quasars also display larger f_c values than radio galaxies (Saikia 1995). Again, B3 J2330+3927, with half of its 8.4 GHz radio emission coming from the core, looks more like a quasar. Therefore, based on its radio morphology, B3 J2330+3927 would be classified as a type I AGN. However, the optical and near-IR Keck spectra (Fig. 5 of DB03) clearly show only narrow emission lines with relatively strong $\text{HeII } \lambda 1640$ and very faint $\text{H}\beta$ typical of type II AGN. Moreover, the optical and near-IR continuum emission is weak and relatively red, as is common in type II AGN.

What is then the most likely explanation for the observed asymmetries in the radio structure of B3 J2330+3927? Up to now, almost all cases of asymmetry in radio galaxies have been explained by environmental effects. In the most detailed study to date, McCarthy et al. (1991) find that for radio-loud type II AGN, the radio lobe closest to the core always lies on the same side of the nucleus as the high surface brightness optical line emission. This is contrary to what is seen in B3 J2330+3927. In fact, Fig. 4 of DB03 shows that the $\text{Ly-}\alpha$ emission extends from the radio core N to the southern radio lobe C, which is almost twice further away from the core than the faint radio lobe A. One could argue that the $\text{Ly-}\alpha$ emission towards lobe A is quenched by dust, which is revealed by its strong far-IR emission (Stevens et al. 2003, DB03). However, the spatial profiles of the non-resonant $[\text{OII}] \lambda 3727$ and $[\text{OIII}] \lambda 5007$ lines in the Keck/NIRC spectra of DB03 show a similar shape, with no emission towards lobe A, indicating that no substantial emission line flux is missing in the $\text{Ly-}\alpha$ profile. Environmental effects thus do not seem to play a major role in the radio morphology of B3 J2330+3927.

If the observed asymmetries are due to relativistic beaming effects, then the fact that B3 J2330+3927 is a clear type II AGN restricts the viewing angle with respect to the line of sight to $\phi > 45^\circ$ (Barthel 1989). However, the fraction of the emission from the nuclear component, $f_c=0.50$ at 8.4 GHz, is very large for a radio galaxy, and suggests the viewing angle must be then close to the $\phi=45^\circ$ limit. If this is case, the obtained arm-length ratio $Q \approx 1.9$ requires a jet velocity of $\beta \approx 0.45c$. Now, the observed ratio of the flux densities of components C and A is $R \gtrsim 11$. If components A and C are optically-thin, isotropically emitting jets, their flux ratio should then be, within the relativistic beaming scenario, $\lesssim 6$ if the jet is made of discrete condensations, or $\lesssim 4$ if it is a continuous jet (an index of $\alpha=-0.9$ has been assumed). Our observed value of $R \gtrsim 11$ is therefore difficult to explain within the standard relativistic beaming framework.

The remaining explanation is an intrinsic difference in the radio jets thus seems to be the most likely explanation of the observed asymmetry. Examples of such radio galaxies are very rare in the literature, and have only been reported at low redshifts. Sources like B3 J2330+3927 and 4C 63.07 are difficult to reconcile with predictions from the standard unified model.

It is also remarkable the lack of increased $\text{Ly-}\alpha$ emission near the region where the radio jet is deflected between

components N and B. In fact, Fig. 2 of PTDB shows a clear change in position angle between the jet-like feature emanating from the core, N, and the line connecting components B1 and B2. However, no increase in the $\text{Ly-}\alpha$ emission is seen in the 2D spectrum (Fig. 4 of DB03), in contrast to similarly deflected radio jets in other HzRGs, showing bright $\text{Ly-}\alpha$ emission at these bendings (e.g., van Ojik et al. 1996).

6. Summary

We have reported on 1.7 and 5.0 GHz VLBA observations of the high-redshift radio galaxy B3 J2330+3927 ($z=3.087$). The combination of these observations with archival 8.4 GHz and 1.4 GHz VLA-A data has helped us interpret the source radio morphology: we have pinpointed the core and jet of the radio galaxy, and discovered a faint counter lobe, which contrary to what has been seen in other radio galaxies lies much farther from the nucleus than the brighter lobe. The values of core-lobe distance ratio and flux density ratio, as well as the fraction of core emission make of B3 J2330+3927 an extremely asymmetric source, and challenges the standard unification model, which explains the differences between quasars and radio galaxies as due to orientation effects.

The results obtained from our VLBA observations of B3 J2330+3927 clearly show that very-long-baseline interferometry (VLBI) observations of HzRGs can contribute crucial information towards a detailed interpretation of the physics of those objects.

Acknowledgements. We thank Robert Laing for stimulating discussions on B3 J2330+3927, and D. Saikia for providing us with the values of R and Q used to produce the diagram in Fig. 3. This research has been partially funded by grant AYA2001-2147-C02-01 of the Spanish Ministerio de Ciencia y Tecnología. MAPT is supported by the programme Ramón y Cajal of the Spanish Ministerio de Educación y Ciencia. The work by WvB at LLNL was performed under the auspices of the U.S. Dept. of Energy and LLNL under contract No. W-7405-Eng-48. The National Radio Astronomy Observatory is a facility of the National Science Foundation operated under cooperative agreement by Associated Universities, Inc. This research has made use of NASA's Astrophysics Data System.

References

- Barthel, P.: 1989, *ApJ*, 336, 606
- Best, P., Bailer, D., Longair, M., Riley, J.: 1995, *MNRAS*, 275, 1171
- Bremer, M. N., Fabian, A. C., Crawford, C. S.: 1997, *MNRAS*, 284, 213
- Carilli, C., Harris, D. E., Pentericci, L., Röttgering, H., Miley, G., Kurk, J.: 2002, *ApJ*, 567, 781
- De Breuck, C., van Breugel, W., Stanford, S. A., Röttgering, H., Miley, G., Stern, D.: 2002 *AJ*, 123, 637
- De Breuck, C., Neri, R., Morganti, R., et al.: 2003, *A&A*, 401, 911
- McCarthy, P., van Breugel, W. & Kapahi, V.: 1991, *ApJ*, 371, 478
- Pacholczyk, A.: 1970, *Radio Astrophysics* (San Francisco: Freeman)
- Pérez-Torres, M. A. & De Breuck, C.: 2005, *MNRAS* (astro-ph/0507489)
- van Ojik R., Röttgering H., Carilli C., Miley G., Bremer, Macchetto D.: 1996, *A&A*, 313, 25

- Saikia, D. J., Jeyakumar, S., Wiita, P. J., Sanghera, H. S., Spencer, R.E.: 1995, MNRAS, 276, 1215
- Saikia, D. J., Jeyakumar, S., Salter, C. J., Thomasson, P., Spencer, R.E., Mantovani, F.: 2001, MNRAS, 321, 37